PROTEIN STRUCTURE REPORT

Solution structure of the E3 ligase HOIL-1 Ubl domain

Steven A. Beasley, Susan S. Safadi, Kathryn R. Barber, and Gary S. Shaw*

Department of Biochemistry, University of Western Ontario, London, Ontario N6A 5C1, Canada

Received 24 January 2012; Accepted 5 April 2012
DOI: 10.1002/pro.2080
Published online 19 April 2012 proteinscience.org

Abstract: The E3 ligases HOIL-1 and parkin are each comprised of an *N*-terminal ubiquitin-like (Ubl) domain followed by a zinc-binding region and *C*-terminal RING–In-between-RING–RING domains. These two proteins, involved in the ubiquitin-mediated degradation pathway, are the only two known E3 ligases to share this type of multidomain architecture. Further, the Ubl domain of both HOIL-1 and parkin has been shown to interact with the S5a subunit of the 26S proteasome. The solution structure of the HOIL-1 Ubl domain was solved using NMR spectroscopy to compare it with that of parkin to determine the structural elements responsible for S5a intermolecular interactions. The final ensemble of 20 structures had a β-grasp Ubl-fold with an overall backbone RMSD of 0.59 ± 0.10 Å in the structured regions between I55 and L131. HOIL-1 had a unique extension of both β1 and β2 sheets compared to parkin and other Ubl domains, a result of a four-residue insertion in this region. A similar 15-residue hydrophobic core in the HOIL-1 Ubl domain resulted in a comparable stability to the parkin Ubl, but significantly lower than that observed for ubiquitin. A comparison with parkin and other Ubl domains indicates that HOIL-1 likely uses a conserved hydrophobic patch (W58, V102, Y127, Y129) found on the β1 face, the β3–β4 loop and β5, as well as a *C*-terminal basic residue (R134) to recruit the S5a subunit as part of the ubiquitin-mediated proteolysis pathway.

Keywords: HOIL-1; parkin; Ubl domain; ubiquitin; S5a; E3 ligase

Introduction

Ubiquitin-like (Ubl) domains are found in numerous proteins involved with protein degradation and signaling that are linked with human diseases such as neurodegeneration (parkin and ubiquilins) and cancer (elongins).[1] One characteristic of many Ubl domains is their ability to interact with the 26S proteasome, predominately through ubiquitin-interacting motifs (UIM)[2] found in the S5a/Rpn10 subunits and Rpn13.[3] Interestingly, the two UIMs in the S5a subunit (UIM1, UIM2) interact preferentially with different Ubls. For example, Ubls from the two human orthologs (hHR23a and hHR23b) of the yeast nucleotide excision repair protein Rad23 bind specifically to UIM2 of the S5a,[4] whereas the Ubl domains

Abbreviations: HOIL-1, heme-oxidized IRP2 ubiquitin ligase 1; LUBAC, linear ubiquitin chain assembly complex; RBR, RING–In-Between-RING–RING; UBA, ubiquitin associated domain; Ubl, ubiquitin-like; UIM, ubiquitin interacting motif.

Additional Supporting Information may be found in the online version of this article.

Steven A. Beasley and Susan S. Safadi contributed equally to this work.

Grant sponsors: Canadian Institutes of Health Research, Canada Research Chairs Program, Canadian Institutes of Health Research Doctoral Scholarship.

**Correspondence to:* Gary S. Shaw, Department of Biochemistry, University of Western Ontario, London, Ontario N6A 5C1, Canada. E-mail: gshaw1@uwo.ca

of hPLIC proteins (orthologs of yeast Dsk2) bind largely to UIM1.[5] The Ubl domain docking to the proteasome provides a mechanism for shuttling ubiquitinated targets for degradation as a ternary complex. The binding of the yeast DdiI Ubl domain to Rpn10 supports this model during the mediated degradation of polyubiquitinated Ho endonuclease,[6] as well as the CIP75 Ubl domain-mediated degradation of the gap junction protein connexion 43.[7] However, not all Ubl domain interactions mediate degradation through the proteasomal pathway, but rather they are involved in other protein–protein interactions as a means of substrate recruitment or regulation. For example, the *N*-terminal Ubl domain of both hHR23a and hPLIC2 can also interact with each other's UBA (ubiquitin-associated domain)[8] providing a mechanism of regulation in the absence of substrates or the proteasome.

The E3 ligase proteins HOIL-1 (heme-oxidized IRP2 ubiquitin ligase) and parkin are both key enzymes involved in the ubiquitin-mediated proteolysis pathway. HOIL-1 was initially characterized as the E3 ligase involved in the regulation of iron metabolism through the heme-binding transcription factor IRP2.[9] HOIL-1 forms a part of the large ~600 kDa heteromeric linear ubiquitin chain assembly complex (LUBAC) that includes another E3 ligase HOIP (HOIL-1 interacting protein) that catalyzes the formation of linear polyubiquitin chains.[10] It is responsible for the linear polyubiquitination of NEMO resulting in the activation of the NF-κB pathway involved in immune and inflammatory responses.[11] Other potential HOIL-1 Ubl domain interacting substrates such as SOCS6[12] and Bach1[13] have been reported as targets of HOIL-1 E3 ligase activity. Parkin has been reported to interact with over 70 different proteins and is thought to regulate processes such as proteasomal degradation, mitochondrial function under stress conditions, and nuclear control of transcription. Mutations in parkin correlate with Autosomal Recessive Juvenile Parkinson's disease[14] and have been shown to cause defects in folding and protein stability as well as disrupting protein interactions.[15,16]

Both the HOIL-1 and parkin enzymes are classified under the RBR E3 ligase family because they both contain a *C*-terminal RING, In-between-RING, RING domain architecture (RBR).[17] Amongst the diverse array of hundreds of RBR E3 ligases, HOIL-1 and parkin are the only two proteins that possess an *N*-terminal Ubl domain followed by an NZF-like zinc-binding domain. The HOIL-1 Ubl domain serves several functions including recruiting substrates for ubiquitination, possibly acting as a shuttle to the proteasome via interaction with the S5a subunit, and interacting with the HOIP UBA domain as a part of LUBAC to mediate the inflammation response. The binding of HOIL-1 to HOIP is crucial for LUBAC formation and activity. The Ubl domain of the E3 ligase parkin has been implicated in shuttling target proteins to the proteasome through an interaction with the S5a UIMs,[18,19] interaction with E2 enzymes or recruiting of putative substrates, which include α-synuclein,[20] Eps15,[21] PDCD2-1,[22] endophillin A,[23] and ataxin-3.[24] One potential mechanism for this is an auto-inhibitory function through intramolecular binding of the Ubl to the E2 binding *C*-terminus, which can be alleviated upon substrate binding.[15] An auto-inhibitory function of an Ubl has also been reported for the deubiquitinating enzyme USP4.[25]

Despite its importance in the ubiquitination pathway and its unique domain architecture, very little structural information is available for HOIL-1 or its E3 ligase relative parkin. In this work, the HOIL-1 Ubl domain was expressed, purified, and its three-dimensional solution structure determined using NMR spectroscopy. The resulting structure was compared to that of the parkin Ubl domain in order to further understand the structural determinants of protein recognition by HOIL-1 with the proteasomal S5a domain.

Results and Discussion

Solution structure of the HOIL-1 Ubl domain

The HOIL-1 Ubl domain (residues 51–139) was expressed in *Escherichia coli* and examined at concentrations at, or below 200 μ*M* since higher concentrations caused precipitation. The resulting ^{1}H-^{15}N-HSQC showed disperse peaks typical of a folded protein (Supporting Information Fig. S1). In particular, 79 of 85 possible backbone amides were visible in the spectrum. Only residues T52, H67, Q100, W101, G104, and L130 were not observable, likely due to exchange with the water. Backbone and side chain assignments were completed using standard triple resonance experiments. The three-dimensional structure of the HOIL-1 Ubl domain (Fig. 1) was determined using 1195 distance restraints measured from ^{15}N-NOESY-HSQC and ^{13}C-NOESY-HSQC spectra, 36 angular restraints derived from Cα, CO, and Hα chemical shifts and 37 hydrogen bond restraints (Table I). The final ensemble of 20 structures had an overall backbone RMSD of 0.59 ± 0.10 Å in the structured regions between I55 and L131. The *N*- and *C*-terminal residues in the HOIL-1 Ubl showed little regular structure. Overall, the structure displays a β-grasp or Ubl-fold having five β-strands (β1, I55-D63; β2, H67-V75; β3, Q100-I103; β4, Q105-L107; β5, N122-L130) and two α helices (α1, V81-Y92 and α2, L114-G118). The β-strands adopt an antiparallel arrangement with the exception of strands β1–β5, which run parallel. A network of hydrogen bonds is found between

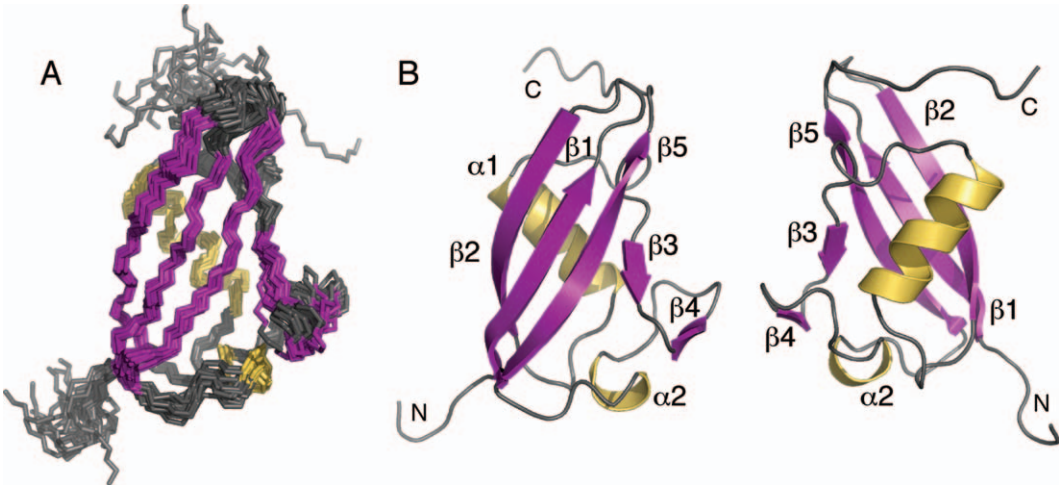

Figure 1. The NMR solution structure of the HOIL-1 Ubl domain. (A) The 20 lowest target function structures were superimposed over residues I55-L131 resulting in a backbone RMSD of 0.59 ± 0.10 Å. (B) Ribbon structures of the representative HOIL-1 Ubl domain are shown in two orientations rotated by 180°. Secondary structured elements are labeled on the ribbon structures, along with α-helices (yellow) and β-sheets (magenta). Structures were analyzed and produced using Pymol (www.pymol.org).

β1–β2 (L57-L73, V59-I71), β1–β5 (R56-G123, W58-D124, W58-A126, S60-A126), β3–β4 (I103-R106), and β3–β5 (V102-Y127). The short β4-strand was the most poorly defined of the five strands consistent with other β-grasp structures. The five β-strands surround the α1 helix that is locked into place by three hydrophobic core residues (V81, L84, V88), which interact with complementary residues (W101; L57; I70, L73, and L128) on the facing β sheets (β3; β1; β2, and β5) and was supported by inter-residue nOes. The representative HOIL-1 structure has a backbone RMSD of 1.70 Å to the parkin Ubl domain and 1.28 Å to ubiquitin. Unsurprisingly, with the large number of common Ubl-folds in the PDB database, a number of significant DALI hits appeared (*Z*-score >2).[26] The HOIL-1 Ubl domain had DALI *Z*-scores of 4.7 and 10.2 to parkin Ubl domain (1IYF) and ubiquitin (1UBQ), respectively highlighting the fold similarity. The HOIL-1 and parkin Ubl domains share 15 conserved hydrophobic residues that comprise the core of the domain from all structured elements (β1-I55, L57, V59; β2-I71, L73, V75; β3-W101, I103; β4-L107; β5-A126, L128; α1-V81, L84, V88; α2-L114) found throughout the sequence (Fig. 2) and are also present in ubiquitin.

HOIL-1 has a hydrophobic binding surface centered at V102 on β3, akin to I44 in parkin and ubiquitin (Fig. 2). There are subtle differences between the Ubl domains with regards to their loop residues and electrostatics that may influence their stabilities, interaction strengths and specificity with proposed target proteins such as S5a. HOIL-1 differs from parkin, and most other Ubl domains, because it has a four amino acid insertion between β1 and β2. This does not increase the loop size between the β-sheets, but rather extends their lengths by two residues at the *C*-terminus of β1 (E62, D63) and one at the *N*-terminus of β2 (T68). This portion of the structure remained well defined due to interactions between these sheets and also with the *C*-terminus of β5. In addition, the HOIL-1 Ubl domain has a shortened loop between β3 and β4 and a longer one between α2 and β5, each differing by one residue

Table I. *Statistics for the 20 Lowest Energy Structures of the HOIL-1 Ubl Domain*

Structural statistics for final structures of HOIL-1 Ubl domain	
Completeness of resonance assignments	
Side chain heavy (512/605)	89.63%
Backbone heavy (242/270)	84.63%
All hydrogens (536/608)	88.16%
Distance and angular restraints	
Total NOE-derived distances	1195
Short ($\|i-j\| = 1$)	607
Medium ($2 \leq \|i-j\| < 5$)	205
Long ($5 \leq \|i-j\|$)	383
Distance restraints per residue	13.6
Dihedral angle restraints[a]	36
H-bond restraints[b]	37
Restraint violations (per structure)	
NOE violations >0.3 Å	0.6
Dihedral constraint violations >2.0°	0
Ramachandran analysis	
Most favored	86.8%
Additionally allowed	13.0%
Generously allowed	0.2%
Disallowed	0%
RMSD to mean structure[c]	
Backbone atoms	0.59 ± 0.10 Å
Heavy atoms	1.16 ± 0.14 Å

[a] Psi/Phi dihedral restraints derived from TALOS.
[b] From ^{1}H-^{15}N-HSQC D_2O exchange experiments.
[c] Structured regions; 55–62, 67–75, 81–92, 101–103, 105–107, 114–117.

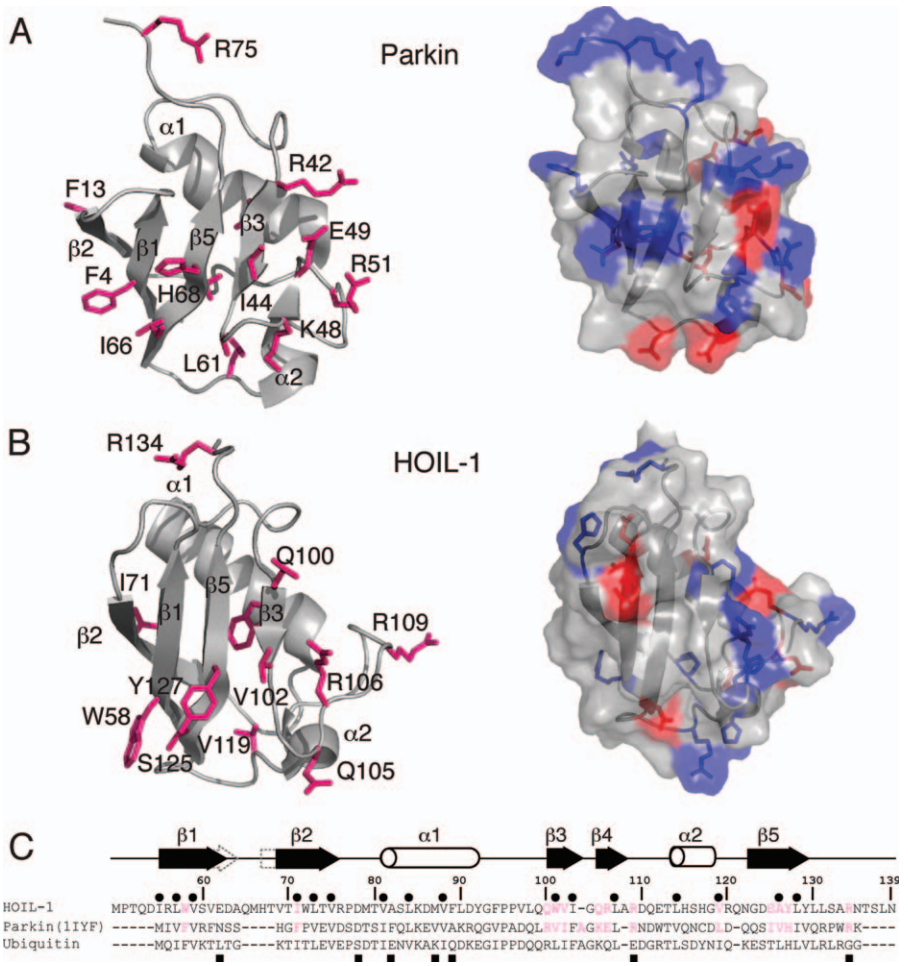

Figure 2. Comparson of HOIL-1 and parkin Ubl structures. Ribbon and charged surface representations of human (A) parkin (1IYF) and (B) HOIL-1 Ubl domains. For parkin, S5a interacting residues (magenta) were determined from observed chemical shift perturbations.[19] For HOIL-1, analogous residues proposed to interact with S5a (magenta) are based on structure-based multiple sequence alignment with parkin and ubiquitin using ClustalW, T-Coffee, and Jalview[27] as shown in (C). Sequence numbering for HOIL-1 is shown with highlighted putative S5a interacting residues indicated (magenta). The observed secondary structures for HOIL-1 and parkin are indicated above the sequences with extended β-sheet structures observed in HOIL-1 indicated by dotted lines. Conserved hydrophobic core residues are indicated above the sequences (•) and positions where charge/hydrophobic residue differences between HOIL-1/parkin and ubiquitin are shown below (■).

compared to parkin. The HOIL-1 Ubl has a minimally charged surface (Fig. 2), a result of three fewer acidic/basic residues compared to parkin and three residues located on the backside of the protein structure with respect to the β-sheets. Four structurally conserved charged residues are present in the HOIL-1 Ubl (D78, K85, R109, R134) compared to parkin (D20, K27, R51, R75). Notably absent from the HOIL-1 surface are basic residues found in parkin on β1 (R6; S60 in HOIL-1), β3 (R42; Q100 in HOIL-1), β4 (K48; Q105 in HOIL-1), and β5 (H68; Y127 in HOIL-1) that form an almost contiguous positively charged surface on parkin. Despite the differences in surface charge, the similarity of the hydrophobic core and fold between HOIL-1 and parkin Ubl domains suggests that their stability should also be comparable. Indeed, thermal unfolding experiments showed that the HOIL-1 and parkin Ubl domains have similar melting midpoints (56 and 63°C, respectively) [Fig. 3(A)]. Interestingly, both proteins are considerably less stable than ubiquitin (85°C) even though the core 15 residues are maintained.

Interacting surface of HOIL-1 Ubl domain with S5a

It has previously been reported that RBCK2, an alternately named splice variant of HOIL-1, interacts with the S5a subunit through its Ubl domain.[28] In our studies, a positive interaction between the HOIL-1 Ubl domain and residues M196-D309 of S5a (His_6-$S5a^{196–309}$) was observed in an affinity assay (Fig. 3). This interaction appeared tighter than that for the parkin Ubl domain with His_6-$S5a^{196–309}$ (Fig. 3) based on approximate band intensities on a gel. The apparent K_d of the parkin Ubl domain with His_6-$S5a^{196–309}$ is about 230 μM,[19] implying the HOIL-1 affinity for S5a is in this range or lower.

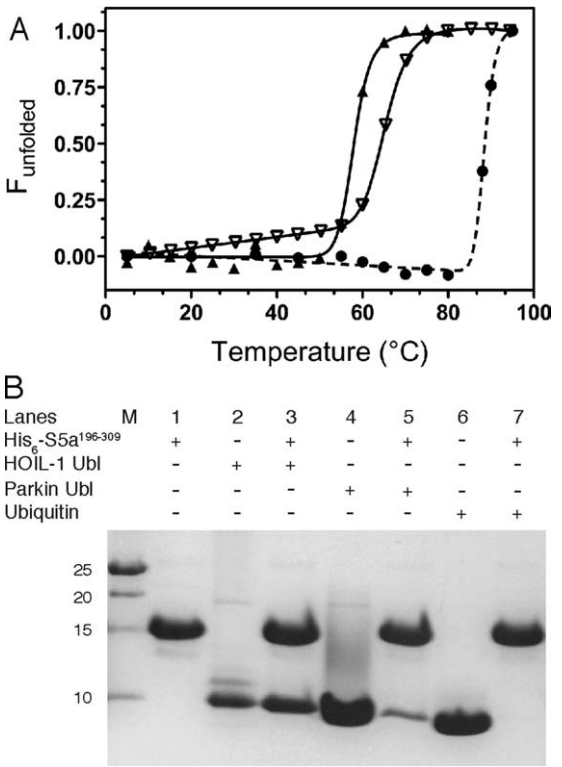

Figure 3. (A) Thermal unfolding experiments for the HOIL-1 Ubl domain (▲), parkin Ubl domain (▽) and ubiquitin (•). The fraction unfolded ($F_{unfolded}$) was calculated using the ellipticity measured at 222 nm from circular dichroism spectropolarimetry experiments. Data were fit using a two-state model, as described in the Materials and Methods section, to determine the midpoints of unfolding[16] for HOIL-1 Ubl (56°C), parkin Ubl (63°C), and ubiquitin (85°C). (B) Affinity experiments showing the interaction of S5a with HOIL-1 Ubl, parkin Ubl, and ubiquitin proteins. The gel shows purified recombinant His_6-S5a$^{196–309}$ (lane 1), HOIL-1 Ubl (lane 2), parkin Ubl (lane 4), and ubiquitin (lane 6) proteins. Samples of His_6-S5a$^{196–309}$ were incubated for 1 h with a Ubl protein, washed twice with binding buffer, and eluted from Ni^{2+}-spin columns with 250 m*M* imidazole (lanes 3, 5, and 7). Samples were resolved by SDS-PAGE and stained with Coomassie Blue. Molecular weight markers are shown (left).

The data also show no observable interaction with ubiquitin, similar to previous reports using affinity experiments,[29] although polyubiquitin chains show a much higher affinity for S5a.[30]

NMR titrations of the HOIL-1 Ubl domain with His_6-S5a$^{196–309}$ were attempted at different salt and pH conditions. Although some changes in line width were noted upon S5a addition, several key residues in the β3–β4 loop (Q100, V102, G104) of HOIL-1, which correspond to residues identified for the parkin-S5a interaction were very weak or not visible in the ^{1}H-^{15}N HSQC spectrum for HOIL-1 making a full chemical shift mapping experiment difficult. To propose a potential S5a interacting site for the HOIL-1 Ubl domain, residues that underwent the largest chemical shift changes in the parkin Ubl[19] upon addition of S5a$^{196–309}$ were mapped to the HOIL-1 structure (Fig. 2) and compared to those residues identified in structures of Ubl-S5a complexes.[20,29,31] In general, there was agreement in residue and structural conservation for several key hydrophobic residues in HOIL-1 (W58, V102, V119) that lie in a similar arrangement as in the parkin Ubl (F4, I44, L61). Interestingly, even though Q105 in HOIL-1 is not conserved by sequence alignment with K48 of parkin, the structure and surface of HOIL-1 shows that the neighboring basic residue (R106) occupies a similar region of space as does K48 in the parkin Ubl domain (Fig. 2). The *C*-terminus of the HOIL-1 Ubl domain contains a positively charged residue (R134) similar to R75 in parkin shown to undergo a significant chemical shift change upon S5a UIM I binding.[19] In hHR23a, this position (K80) is located near two glutamates (E283, E285) in the S5a UIM II[32] whereas distinct contacts with conserved negatively charged residues on the SH3 domain of endophilin-A are found near this residue (R75) in parkin.[23] There are some differences in the surface hydrophobic residues in HOIL-1 compared to parkin that might impact its tighter binding to S5a observed in our affinity experiments. For example, V102, Y127, and Y129 in HOIL-1 are occupied by I44, H68, and V70 in parkin. Overall, although the structure of the HOIL-1 Ubl is similar to that of parkin, the two proteins are distinguished by different distributions of hydrophobic and charged residues that likely contribute to the observed binding differences between HOIL-1 and parkin for the S5a subunit.

Materials and Methods

Cloning, protein expression, and purification

A cDNA encoding human HOIL-1 domain (ATCC 10700493) was used to clone a fragment encoding the Ubl (residues 51–139) into the NdeI and BamHI sites of a pET21a vector (Novagen). The HOIL-1 Ubl protein was overexpressed in the BL21(DE3) Codon Plus RIL *E. coli* strain. The bacteria were grown at 37°C overnight in 2xYT media (10 mL) containing ampicillin (50 μg/mL) and chloramphenicol (34 μg/mL). The culture was diluted 1:100 in 2xYT media (10 mL in 1 L) containing the same antibiotics. Expression was induced at an OD_{600} of 0.6–0.7 by the addition of 1 m*M* IPTG and allowed to grow overnight at 15°C with constant shaking. For the production of ^{15}N-^{13}C-labeled proteins, cells were grown in M9 minimal media containing 1.0 g/L $^{15}NH_4Cl$ and 2.0 g/L ^{13}C-glucose. The protein was purified as previously described for the parkin Ubl.[33] The integrity of the protein was confirmed by electrospray ionization mass spectrometry (UWO Biological Mass Spectrometry Laboratory).

NMR spectroscopy

All NMR experiments were performed on Varian Inova 600 MHz NMR spectrometers equipped with either a ^{13}C-enhanced triple resonance cold probe with *z*-gradients or an *xyz* gradient, triple resonance probe (Biomolecular NMR Facility, UWO). HOIL-1 Ubl samples were concentrated to ~200 μ*M* in 10 m*M* KH_2PO_4, 1 m*M* EDTA, 50 m*M* KCl, 30 μ*M* DSS, 90% H_2O/10% D_2O at pH 7.0. Ubl samples in D_2O were repeatedly concentrated and resuspended in the same buffer prepared with D_2O. For backbone chemical shift assignments, sensitivity-enhanced ^{1}H-^{15}N-HSQC and complementary HNCO/HN(CA)CO,[34,35] HNCA/HN(CO)CA,[34,35] HNCACB/CBCA(CO)NH[36,37] experiments were performed. Side chain resonances were completed using C(CO)NH,[38] HC(CO)NH,[38] and HCCH-TOCSY[39] experiments. NOE-derived distance restraints were obtained from aromatic and aliphatic ^{13}C-NOESY-HSQC experiments (100 ms)[40] collected in D_2O and a ^{15}N-NOESY-HSQC (150 ms)[41] collected in 90% H_2O/10% D_2O. All spectra were processed with NMRPipe[42] software using a 60° shifted, cosine-squared function in all dimensions and analyzed using NMRView.[43] Chemical shift assignments have been deposited to the BMRB (accession 17828).

Structure calculations

The structure determination of the HOIL-1 Ubl domain was completed using CYANA 2.1[44] in combination with manually and automatically assigned nOes from NOESY spectra, angular restraints as predicted from the TALOS+ server and hydrogen bonding information from qualitative amide exchange experiments. Distance calibrations and parameterization, as previously described,[45] were used to complete seven iterations of refinement of 100 structures per cycle, with the 20 structures having the lowest calculated target function from each cycle used to seed the next round for further automated NOE assignment. Angular restraints (ϕ, ψ) with a minimum range of ± 20° were included in spans of at least three sequential residues that were scored as "GOOD" by TALOS+.[46] After the initial fold of the protein had been identified from structure calculations, hydrogen bond restraints were added to the calculation based on the presence of peaks in the ^{1}H-^{15}N-HSQC after 7 days of D_2O exchange and the observation of close amide, carbonyl oxygen atoms in preliminary calculated structures. The final 20 structures with the lowest target function were chosen as representative of the calculation, although structures with higher target values had nearly identical folds. Water refinement was completed on the ensemble using XPLOR-NIH and energy minimization using modified RECOORD scripts.[47] Validation of the structures was performed using PROCHECK[48] and WHATCHECK.[49] The family of 20 structures has been deposited to the Protein Data Bank under accession code 2LGY.

Protein stability and interaction experiments

Unfolding experiments were conducted by thermal denaturation using circular dichroism on a Jasco J-810 instrument (Biomolecular Interactions and Conformations Facility, University of Western Ontario). Protein concentrations ranged from 20 to 80 μ*M*. The temperature was increased from 5 to 80°C at both 30 and 50°C per hour. The data were converted to fraction unfolded using $F_{\text{unfolded}} = (\theta_{\text{obs}} - \theta_{\text{max}})/(\theta_{\text{max}} - \theta_{\text{min}})$, where θ_{obs} is the observed CD signal at 222 nm, θ_{max} is the signal for the folded protein, and θ_{min} is the signal for the unfolded protein. A two-state unfolding curve was used to fit the F_{unfolded} as a function of temperature as previously described.[16]

S5a binding assays were completed using purified His-S5a$^{196–309}$ protein mixed with either purified HOIL-1 Ubl, parkin Ubl, or ubiquitin proteins. Typically, a 1:2 molar ratio of S5a: Ubl was incubated for 1 h at 4°C in 10 m*M* imidazole in 20 m*M* Na_2HPO_4, 300 m*M* NaCl, pH 8.0 prior to loading onto a Ni-NTA column. Columns were washed twice with the same buffer and eluted using 250 m*M* imidazole in 20 m*M* Na_2HPO_4, 300 m*M* NaCl, pH 8.0.[16]

Acknowledgments

The authors thank Dr. Pascal Mercier, Dr. Don Spratt, Jane Bai, and Elio Cino for their insightful comments and assistance.

References

1. Madsen L, Schulze A, Seeger M, Hartmann-Petersen R (2007) Ubiquitin domain proteins in disease. BMC Biochem 8 (Suppl 1):S1.
2. Hofmann K, Falquet L (2001) A ubiquitin-interacting motif conserved in components of the proteasomal and lysosomal protein degradation systems. Trends Biochem Sci 26:347–350.
3. Su V, Lau AF (2009) Ubiquitin-like and ubiquitin-associated domain proteins: significance in proteasomal degradation. Cell Mol Life Sci 66:2819–2833.
4. Hiyama H, Yokoi M, Masutani C, Sugasawa K, Maekawa T, Tanaka K, Hoeijmakers JH, Hanaoka F (1999) Interaction of hHR23 with S5a. The ubiquitin-like domain of hHR23 mediates interaction with S5a subunit of 26S proteasome. J Biol Chem 274:28019–28025.
5. Ko HS, Uehara T, Tsuruma K, Nomura Y (2004) Ubiquilin interacts with ubiquitylated proteins and proteasome through its ubiquitin-associated and ubiquitin-like domains. FEBS Lett 566:110–114.
6. Kaplun L, Tzirkin R, Bakhrat A, Shabek N, Ivantsiv Y, Raveh D (2005) The DNA damage-inducible UbL-UbA protein Ddi1 participates in Mec1-mediated degradation of Ho endonuclease. Mol Cell Biol 25:5355–5362.
7. Li X, Su V, Kurata WE, Jin C, Lau AF (2008) A novel connexin43-interacting protein, CIP75, which belongs to the UbL-UBA protein family, regulates the turnover of connexin 43. J Biol Chem 283:5748–5759.

8. Kang Y, Zhang N, Koepp DM, Walters KJ (2007) Ubiquitin receptor proteins hHR23a and hPLIC2 interact. J Mol Biol 365:1093–1101.
9. Yamanaka K, Ishikawa H, Megumi Y, Tokunaga F, Kanie M, Rouault TA, Morishima I, Minato N, Ishimori K, Iwai K (2003) Identification of the ubiquitin-protein ligase that recognizes oxidized IRP2. Nat Cell Biol 5: 336–340.
10. Kirisako T, Kamei K, Murata S, Kato M, Fukumoto H, Kanie M, Sano S, Tokunaga F, Tanaka K, Iwai K (2006) A ubiquitin ligase complex assembles linear polyubiquitin chains. EMBO J 25:4877–4887.
11. Tokunaga F, Sakata S, Saeki Y, Satomi Y, Kirisako T, Kamei K, Nakagawa T, Kato M, Murata S, Yamaoka S, Yamamoto M, Akira S, Takao T, Tanaka K, Iwai K (2009) Involvement of linear polyubiquitylation of NEMO in NF-κB activation. Nat Cell Biol 11:123–132.
12. Bayle J, Lopez S, Iwai K, Dubreuil P, De Sepulveda P (2006) The E3 ubiquitin ligase HOIL-1 induces the polyubiquitination and degradation of SOCS6 associated proteins. FEBS Lett 580:2609–2614.
13. Zenke-Kawasaki Y, Dohi Y, Katoh Y, Ikura T, Ikura M, Asahara T, Tokunaga F, Iwai K, Igarashi K (2007) Heme induces ubiquitination and degradation of the transcription factor Bach1. Mol Cell Biol 27:6962–6971.
14. Kitada T, Asakawa S, Hattori N, Matsumine H, Yamamura Y, Minoshima S, Yokochi M, Mizuno Y, Shimizu N (1998) Mutations in the parkin gene cause autosomal recessive juvenile parkinsonism. Nature 392:605–608.
15. Chaugule VK, Burchell L, Barber KR, Sidhu A, Leslie SJ, Shaw GS, Walden H (2011) Autoregulation of Parkin activity through its ubiquitin-like domain. EMBO J 30:2853–2867.
16. Safadi SS, Barber KR, Shaw GS (2011) Impact of autosomal recessive juvenile Parkinson's disease mutations on the structure and interactions of the parkin ubiquitin-like domain. Biochemistry 50:2603–2610.
17. Marin I (2009) RBR ubiquitin ligases: diversification and streamlining in animal lineages. J Mol Evol 69: 54–64.
18. Sakata E, Yamaguchi Y, Kurimoto E, Kikuchi J, Yokoyama S, Yamada S, Kawahara H, Yokosawa H, Hattori N, Mizuno Y, Tanaka K, Kato K (2003) Parkin binds the Rpn10 subunit of 26S proteasomes through its ubiquitin-like domain. EMBO Rep 4:301–306.
19. Safadi SS, Shaw GS (2010) Differential interaction of the E3 ligase parkin with the proteasomal subunit S5a and the endocytic protein Eps15. J Biol Chem 285: 1424–1434.
20. Shimura H, Schlossmacher MG, Hattori N, Frosch MP, Trockenbacher A, Schneider R, Mizuno Y, Kosik KS, Selkoe DJ (2001) Ubiquitination of a new form of α-synuclein by parkin from human brain: implications for Parkinson's disease. Science 293:263–269.
21. Fallon L, Belanger CM, Corera AT, Kontogiannea M, Regan-Klapisz E, Moreau F, Voortman J, Haber M, Rouleau G, Thorarinsdottir T, Brice A, van Bergen En Henegouwen PM, Fon EA (2006) A regulated interaction with the UIM protein Eps15 implicates parkin in EGF receptor trafficking and PI(3)K-Akt signalling. Nat Cell Biol 8:834–842.
22. Fukae J, Sato S, Shiba K, Sato K, Mori H, Sharp PA, Mizuno Y, Hattori N (2009) Programmed cell death-2 isoform1 is ubiquitinated by parkin and increased in the substantia nigra of patients with autosomal recessive Parkinson's disease. FEBS Lett 583:521–525.
23. Trempe JF, Chen CX, Grenier K, Camacho EM, Kozlov G, McPherson PS, Gehring K, Fon EA (2009) SH3 domains from a subset of BAR proteins define a Ubl-binding domain and implicate parkin in synaptic ubiquitination. Mol Cell 36:1034–1047.
24. Durcan TM, Kontogiannea M, Thorarinsdottir T, Fallon L, Williams AJ, Djarmati A, Fantaneanu T, Paulson HL, Fon EA (2011) The Machado-Joseph disease-associated mutant form of ataxin-3 regulates parkin ubiquitination and stability. Hum Mol Genet 20:141–154.
25. Luna-Vargas MP, Faesen AC, van Dijk WJ, Rape M, Fish A, Sixma TK (2011) Ubiquitin-specific protease 4 is inhibited by its ubiquitin-like domain. EMBO Rep 12:365–372.
26. Holm L, Kaariainen S, Rosenstrom P, Schenkel A (2008) Searching protein structure databases with DaliLite v.3. Bioinformatics 24:2780–2781.
27. Waterhouse AM, Procter JB, Martin DM, Clamp M, Barton GJ (2009) Jalview Version 2—a multiple sequence alignment editor and analysis workbench. Bioinformatics 25:1189–1191.
28. Yoshimoto N, Tatematsu K, Okajima T, Tanizawa K, Kuroda S (2009) Accumulation of polyubiquitinated proteins by overexpression of RBCC protein interacting with protein kinase C2, a splice variant of ubiquitin ligase RBCC protein interacting with protein kinase C1. FEBS J 276:6375–6385.
29. Wang Q, Young P, Walters KJ (2005) Structure of S5a bound to monoubiquitin provides a model for polyubiquitin recognition. J Mol Biol 348:727–739.
30. Young P, Deveraux Q, Beal RE, Pickart CM, Rechsteiner M (1998) Characterization of two polyubiquitin binding sites in the 26S protease subunit S5a. J Biol Chem 273:5461–5467.
31. Walters KJ, Kleijnen MF, Goh AM, Wagner G, Howley PM (2002) Structural studies of the interaction between ubiquitin family proteins and proteasome subunit S5a. Biochemistry 41:1767–1777.
32. Mueller TD, Feigon J (2003) Structural determinants for the binding of ubiquitin-like domains to the proteasome. EMBO J 22:4634–4645.
33. Safadi SS, Shaw GS (2007) A disease state mutation unfolds the parkin ubiquitin-like domain. Biochemistry 46:14162–14169.
34. Ikura M, Kay LE, Bax A (1990) A novel approach for sequential assignment of proton, carbon-13, and nitrogen-15 spectra of larger proteins:heteronuclear triple-resonance three-dimensional NMR spectroscopy. Biochemistry 29:4659–4667.
35. Yamazaki T, Lee W, Arrowsmith CH, Muhandiram DR, Kay LE (1994) A suite of triple resonance NMR experiments for the backbone assignment of ^{15}N, ^{13}C, ^{2}H labeled proteins with high sensitivity. J Am Chem Soc 116:11655–11666.
36. Wittekind M, Mueller L (1993) HNCACB, a high-sensitivity 3D NMR experiment to correlate amide-proton and nitrogen resonances with the α- and β-carbon resonances in proteins. J Magn Reson B 101:201–205.
37. Grzesiek S, Bax A (1992) Correlating backbone amide and side chain resonances in larger proteins by multiple relayed triple resonance NMR. J Am Chem Soc 114:6291–6293.
38. Grzesiek S, Anglister J, Bax A (1993) Correlation of backbone amide and aliphatic side-chain resonances in $^{13}C/^{15}N$-enriched proteins by isotopic mixing of ^{13}C magnetization. J Magn Reson B 101:114–119.
39. Kay LE, Xu G, Singer AU, Muhandiram DR, Forman-Kay JD (1993) A gradient-enhanced HCCH-TOCSY experiment for recording sidechain ^{1}H and ^{13}C correlations in H_2O samples of proteins. J Magn Reson 101:333–337.
40. Zhang O, Kay LE, Olivier JP, Forman-Kay JD (1994) Backbone ^{1}H and ^{15}N resonance assignments of the

N-terminal SH3 domain of drk in folded and unfolded states using enhanced-sensitivity pulsed field gradient NMR techniques. J Biomol NMR 4:845–858.
41. Muhandiram DR, Farrow NA, Xu G-Y, Smallcombe SH, Kay LE (1993) A gradient ^{13}C NOESY-HSQC experiment for recording NOESY spectra of ^{13}C-labeled proteins dissolved in H_2O. J Magn Reson 102:317–321.
42. Delaglio F, Grzesiek S, Vuister GW, Zhu G, Pfeifer J, Bax A (1995) NMRPipe: a multidimensional spectral processing system based on UNIX pipes. J Biomol NMR 6:277–293.
43. Johnson BA (2004) Using NMRView to visualize and analyze the NMR spectra of macromolecules. Methods Mol Biol 278:313–352.
44. Guntert P, Mumenthaler C, Wuthrich K (1997) Torsion angle dynamics for NMR structure calculation with the new program DYANA. J Mol Biol 273:283–298.
45. Herrmann T, Guntert P, Wuthrich K (2002) Protein NMR structure determination with automated NOE assignment using the new software CANDID and the torsion angle dynamics algorithm DYANA. J Mol Biol 319:209–227.
46. Shen Y, Delaglio F, Cornilescu G, Bax A (2009) TALOS+: a hybrid method for predicting protein backbone torsion angles from NMR chemical shifts. J Biomol NMR 44:213–223.
47. Nederveen AJ, Doreleijers JF, Vranken W, Miller Z, Spronk CA, Nabuurs SB, Guntert P, Livny M, Markley JL, Nilges M, Ulrich EL, Kaptein R, Bonvin AM (2005) RECOORD: a recalculated coordinate database of 500+ proteins from the PDB using restraints from the BioMagResBank. Proteins 59:662–672.
48. Laskowski RA, MacArthur M, Moss DS, Thornton JM (1993) PROCHECK: a program to check the stereochemical quality of protein structures. J Appl Cryst 26: 283–291.
49. Hooft RW, Vriend G, Sander C, Abola EE (1996) Errors in protein structures. Nature 381:272.